THE ASTROPHYSICAL JOURNAL, 531:693–700, 2000 March 10

CYCLIC CHANGES IN DUST-TO-GAS RATIO

HIROYUKI HIRASHITA[1,2]

Received 1999 June 16; accepted 1999 October 19

ABSTRACT

We discuss the time variation of the dust-to-gas mass ratio in spiral galaxies, using the multiphase model of interstellar medium. The typical timescale of the phase change of an interstellar gas is $\sim 10^{7-8}$ yr in spiral galaxies. Since the phase transition changes the filling factor of the cold gas where the dust growth occurs, the dust growth rate varies on that timescale. In order to examine the response of the dust-to-gas ratio to the phase transition, we construct a model of the time evolution of the dust-to-gas ratio. We adopt the three-phase model for the interstellar gas and the Ikeuchi-Tomita model for the mass exchange between the phases. According to the model, three types of solutions are possible: (1) all the gas is transformed to a hot gas; (2) a stable stationary state of three phases is realized; and (3) the filling factor of each phase cyclically changes. For the three types of solutions, the dust-to-gas ratio behaves as follows: for solution 1, almost all the dust is destroyed (the dust-to-gas ratio becomes ~ 0); for solution 2, the dust-to-gas ratio converges to a stationary state; and for solution 3, the dust-to-gas ratio varies cyclically in response to the phase transition. In the case of solution 3, the amplitude of the variation of the dust-to-gas ratio is large (nearly an order of magnitude) if the dust growth timescale is shorter than the phase transition timescale. This condition is easily satisfied in spiral galaxies. However, it is difficult for dwarf galaxies to realize the condition, because their small metallicity makes the dust growth timescale long.

Subject headings: galaxies: evolution — galaxies: ISM — galaxies: spiral

1. INTRODUCTION

Some of the recent chemical evolution models of galaxies have successfully included the dust content (Wang 1991; Lisenfeld & Ferrara 1998; Dwek 1998; Hirashita 1999a, hereafter H99). Takagi, Arimoto, & Vansevičius (1999) modeled the dust extinction in ultraviolet–optical wavelengths and the reprocessed light in the far-infrared (FIR) region, presenting the spectral evolution in the UV–FIR wavelengths.

As to the dust formation, supernovae (SNe) are known to be one of the most dominant sources (Barlow 1978; Draine & Salpeter 1979; Dwek & Scalo 1980), and SN shocks destroy grains (McKee et al. 1987; Jones et al. 1994; Borkowski & Dwek 1995). Thus, dust content is connected with star formation histories. In our previous work, H99, the dust-to-gas mass ratio is expressed as a nonlinear function of metallicity, which is also related to star formation histories (see also Lisenfeld & Ferrara 1998). H99 confirmed the suggestion proposed by Dwek (1998) that the process of accretion onto preexisting dust grains is efficient in spiral galaxies. This is also supported by the observations of elemental depletions in dense clouds (e.g., Draine 1990). Since the accretion is effective in cold clouds, the global efficiency of the accretion depends on the fractional mass of the cold gas (Seab 1987; McKee 1989; Draine 1990; Hirashita 1999b). Thus, the efficiency varies on the timescale of the phase transition of the interstellar medium (ISM; $\sim 10^{7-8}$ yr; Ikeuchi 1988; McKee 1989).

McKee & Ostriker (1977) constructed a standard model for the ISM that is composed of three phases: the hot rarefied gas ($T \sim 10^6$ K and $n \sim 10^{-3}$ cm^{-3}), the warm gas ($T \sim 10^4$ K and $n \sim 10^{-1}$ cm^{-3}), and the cold cloud ($T \sim 10^2$ K and $n \sim 10$ cm^{-3}). One of the simplest models for the mass exchange between the three ISM phases is described by Ikeuchi & Tomita (1983, hereafter IT83; see also Habe, Ikeuchi, & Tanaka 1981). They included the following three processes: (1) the sweeping of a warm gas into a cold component, (2) the evaporation of cold clouds embedded in a hot gas, and (3) the radiative cooling of a hot gas by collisions with a warm gas. The mass fraction of each component can show an oscillatory behavior, which is known as a limit cycle (Nicolis & Prigogine 1977; see also Fujimoto & Ikeuchi 1984 for another modeling of interstellar gas). The limit-cycle behavior is supported by Kamaya & Takeuchi (1997, hereafter KT97), who interpreted the various levels of the star formation activities in spiral galaxies shown by Tomita, Tomita, & Saitō (1996) using the limit-cycle model.

In the limit-cycle model by IT83, the mass fraction of each phase oscillates continuously because of the mass exchange between the three components of the ISM (see also Korchagin, Ryabtsev, & Vorobyov 1994). The timescale of the phase transition in the model is determined by the three timescales of the above physical processes 1–3. Actually, a static solution, as well as the limit-cycle solution for the mass fractions, is possible for some range in the parameter space (this case is also examined in this paper). However, the oscillatory behavior (i.e., the limit-cycle model) of the fractional masses is supported observationally. Indeed, the observed scatter of the FIR-to-optical flux ratios of spiral galaxies (Tomita et al. 1996) is interpreted through the limit-cycle model in KT97, who suggested that the fractional mass of the cold phase changes in the range of 0.1– 0.7 (or more) on the timescale of 10^{7-8} yr and that this leads to the time variation of star formation activities if the Schmidt law (Schmidt 1959) is applicable.

Hirashita (1999b) combined the framework of H99 with a theoretical work on multiphase ISM and suggested the time

[1] Department of Astronomy, Faculty of Science, Kyoto University, Sakyo-ku, Kyoto 606-8502, Japan; hirasita@kusastro.kyoto-u.ac.jp.
[2] Research Fellow of the Japan Society for the Promotion of Science.

variation of the dust-to-gas ratio by the phase transition. We aim at constructing a model of the time evolution of the dust-to-gas ratio including the effect of the ISM phase transition. The model in this paper enables us to simulate the time variation of the dust-to-gas ratio in a galaxy. This paper is organized as follows. First, in the next section, a model for the time variation of the dust-to-gas ratio is presented. Next, we show the numerical solution of the model in § 3. In § 4, we discuss the solution and present observational implications. Finally, § 5 is devoted to summary.

2. MODELING OF DUST-TO-GAS RATIO AND ISM PHASE TRANSITION

2.1. *Dust-to-Gas Ratio*

First, we prepare a model for the time variation of the dust-to-gas ratio in a galaxy. The model was developed by H99 (see also Lisenfeld & Ferrara 1998 and Dwek 1998) in order to account for the relation between the metallicities and the dust-to-gas ratios of nearby spiral galaxies. In H99, we adopted a simple one-zone model (i.e., the galaxy is treated as a closed system and spatial variations of physical quantities within the galaxy are neglected). The model's equations describe the rates of change in the masses of gas, metal, and dust:

$$\frac{dM_g}{dt} = -\psi + E \,, \tag{1}$$

$$\frac{dM_i}{dt} = -X_i\psi + E_i \,, \tag{2}$$

$$\frac{dM_{d,i}}{dt} = f_{\mathrm{in},i}E_i - \alpha f_i X_i \psi + \frac{M_{d,i}(1-f_i)}{\tau_{\mathrm{acc}}} - \frac{M_{d,i}}{\tau_{\mathrm{SN}}} \,. \tag{3}$$

Here M_g is the mass of gas; M_i and $M_{d,i}$, respectively, denote the total masses of the metal i (i = O, C, Si, Mg, Fe, etc.) in both gas and dust phases, and only in the dust phase. The star formation rate is denoted by ψ; E is the rate of the total injection of mass from stars; X_i is the mass fraction of the element i (i.e., $X_i \equiv M_i/M_g$); E_i is the rate of the total injection of element i from stars; and f_i is the mass fraction of the element i locked up in dust (i.e., $f_i = M_{d,i}/M_i$). The meanings of the other parameters in the above equations are as follows: $f_{\mathrm{in},i}$ represents the dust mass fraction in the injected material (in other words, the dust condensation efficiency in the ejecta such as stellar winds or SNe); α refers to the efficiency of dust destruction during star formation [$\alpha = 1$ corresponds to destruction of only the dust incorporated into the star, and $\alpha > 1$ ($\alpha < 1$) corresponds to a net destruction (formation) in the star formation]; τ_{acc} is the timescale of accretion of the element i onto preexisting dust grains in molecular clouds; and τ_{SN} is the timescale of dust destruction by SN shocks. We hereafter assume that only dust incorporated into stars is destroyed when the stars form; i.e., $\alpha = 1$. The mass loss from the galaxy is neglected in this paper, since we mainly treat spiral galaxies and expect that outflows are prevented by their deep dark matter potentials (Habe & Ikeuchi 1980). When we consider starburst-phase (Habe & Ikeuchi 1980) or dwarf galaxies (Mac Low & Ferrara 1999), the outflows may be important for the dust content as well as gas and metal content (Lisenfeld & Ferrara 1998).

We adopt the instantaneous recycling approximation (i.e., a star with mass larger than m_1 dies instantaneously after its birth, leaving the remnant of mass w_m). Once the initial mass function is fixed, we can calculate the returned fraction of the mass from formed stars ($\mathcal{R}$) and the mass fraction of the element i that is newly produced and ejected by stars ($\mathcal{Y}_i$). Using $\mathcal{R}$ and $\mathcal{Y}_i$, we write E and E_i in equations (1)–(3) as (see H99 for the details)

$$E = \mathcal{R}\psi \,, \tag{4}$$

$$E_i = (\mathcal{R}X_i + \mathcal{Y}_i)\psi \,. \tag{5}$$

After some algebra, equations (2) and (3) become

$$\tau_{\mathrm{SF}}\frac{dX_i}{dt} = \mathcal{Y}_i \,, \tag{6}$$

$$\tau_{\mathrm{SF}}\frac{d\mathcal{D}_i}{dt} = f_{\mathrm{in},i}(\mathcal{R}X_i + \mathcal{Y}_i) - [\alpha - 1 + \mathcal{R} - \beta_{\mathrm{acc}}(1-f_i) + \beta_{\mathrm{SN}}]\mathcal{D}_i \,, \tag{7}$$

where $\tau_{\mathrm{SF}} \equiv M_g/\psi$ (timescale of gas consumption; e.g., Roberts 1963), $\mathcal{D}_i \equiv M_{d,i}/M_g = f_i X_i$, $\beta_{\mathrm{acc}} \equiv \tau_{\mathrm{SF}}/\tau_{\mathrm{acc}}$, and $\beta_{\mathrm{SN}} \equiv \tau_{\mathrm{SF}}/\tau_{\mathrm{SN}}$. The timescales above are estimated in the case of typical spiral galaxies as $\tau_{\mathrm{SF}} \sim$ 1–10 Gyr (Kennicutt, Tamblyn, & Congdon 1994) and $\tau_{\mathrm{acc}} \sim \tau_{\mathrm{SN}} \sim 10^8$ yr (Draine 1990).

The two timescales, τ_{acc} and τ_{SN}, depend on the phase of the ISM where the dust exists (Draine 1990; Hirashita 1999b). The accretion timescale, τ_{acc}, is shorter in the cold phase of the ISM than in any other phase, since efficient accretion requires a dense environment. If we express the growth timescale of a dust grain in the cold component as τ_{grow}, the accretion timescale is expressed as $\tau_{\mathrm{acc}} = \tau_{\mathrm{grow}}/X_{\mathrm{cold}}$, where X_{cold} represents the mass fraction of the cold phase to the total mass of ISM (Hirashita 1999b). This is equivalent to

$$\beta_{\mathrm{acc}} = X_{\mathrm{cold}}\beta_{\mathrm{grow}} \,, \tag{8}$$

where $\beta_{\mathrm{grow}} \equiv \tau_{\mathrm{SF}}/\tau_{\mathrm{grow}}$. According to Draine (1990), $\tau_{\mathrm{grow}} \sim 5 \times 10^7$ yr in the cold gas. The destruction timescale of the dust β_{SN} is kept constant for simplicity, since we would like to concentrate on the time variation of the dust growth efficiency to examine the result in Hirashita (1999b). The star formation history should be taken into account in order to model the time dependence of β_{SN}. Moreover, the time variation of the SN rate also contributes to the time variation of the fractional masses the three ISM components. Because of such complexities in the time dependence of β_{SN}, we simply treat β_{SN} as constant.

2.2. *ISM Phase Transition*

Next, we review the model by IT83. This model is used to calculate the time evolution of the filling factors of the three ISM phases (see also § 1). The result is used to calculate the dust formation efficiency through equation (8).

The interstellar medium is assumed to consist of three components (McKee & Ostriker 1977): the hot rarefied gas ($T \sim 10^6$ K, $n \sim 10^{-3}$ cm^{-3}), the warm gas ($T \sim 10^4$ K, $n \sim 10^{-1}$ cm^{-3}), and the cold cloud ($T \sim 10^2$ K, $n \sim 10$ cm^{-3}). The fractional masses of the three components are X_{hot}, X_{warm}, and X_{cold}, respectively. A trivial relation is

$$X_{\mathrm{hot}} + X_{\mathrm{warm}} + X_{\mathrm{cold}} = 1 \,. \tag{9}$$

The following three processes are considered (see IT83 for the details): (1) the sweeping of a warm gas into a cold

component at the rate of $aX_{\rm warm}$ ($a \sim 5 \times 10^{-8}$ yr^{-1}); (2) the evaporation of cold clouds embedded in a hot gas at the rate of $bX_{\rm cold}X_{\rm hot}^2$ ($b \sim 10^{-7}$–10^{-8} yr^{-1}); (3) the radiative cooling of a hot gas through collisions with a warm gas at the rate of $cX_{\rm warm}X_{\rm hot}$ ($c \sim 10^{-6}$–10^{-7} yr^{-1}). Writing down the rate equations and using equation (9), we obtain

$$\frac{dX_{\rm cold}}{d\tau} = -BX_{\rm cold}X_{\rm hot}^2 + A(1 - X_{\rm cold} - X_{\rm hot}) , \quad (10)$$

$$\frac{dX_{\rm hot}}{d\tau} = -X_{\rm hot}(1 - X_{\rm cold} - X_{\rm hot}) + BX_{\rm cold}X_{\rm hot}^2 , \quad (11)$$

where $\tau \equiv ct$, $A \equiv a/c$, and $B \equiv b/c$.

The solutions of equations (10) and (11) are classified into the following three types (IT83):

1. $A > 1$: all the orbits in the ($X_{\rm cold}$, $X_{\rm hot}$) plane reduce to the node (0, 1),
2. $A < 1$ and $B > B_{\rm cr}$: all the orbits reduce to a stable focus $[(1 - A)/(AB + 1), A]$,
3. $A < 1$ and $B < B_{\rm cr}$: all the orbits converge on a limit-cycle orbit,

where $B_{\rm cr} \equiv (1 - 2A)/A^2$. As representative parameter sets for solution types 1 and 2, we examine $(A, B) = (1.2, 3.0)$ and $(A, B) = (0.4, 3.0)$, respectively (denoted in Table 1 as models 1 and 2, respectively). We especially concentrate on case 3, since we treat spiral galaxies with cold gas and with various levels of star formation activities (e.g., Tomita et al. 1996). The two properties of spiral galaxies are naturally realized (KT97) if the filling factor of the cold gas shows the limit-cycle behavior and the star formation rate changes according to the Schmidt law ($\psi \propto X_{\rm cold}^n$; n = 1–2; Schmidt 1959). As representative parameter sets of the limit-cycle orbit, we examine the cases of $(A, B) = (0.3, 3.0)$ and $(A, B) = (0.3, 0.5)$ (denoted in Table 1 by models 3 and 4, respectively).[3] The cycle period of the former case is about 3 times shorter than that of the latter.

In Table 1, the adopted parameters are summarized. The "Type" column refers to the behaviors of the solutions, which are named "Runaway," "Stationary," and "Limit-Cycle" for cases 1, 2, and 3, respectively. We note that all the parameter sets above are examined in IT83 (their Figures 1 and 3).

2.3. *Summary of the Basic Equations*

Here, we summarize the equations and the parameters. First, the filling factor of the cold gas is calculated by the following set of equations:

$$\frac{dX_{\rm cold}}{d\tau} = -BX_{\rm cold}X_{\rm hot}^2 + A(1 - X_{\rm cold} - X_{\rm hot}) , \quad (12)$$

$$\frac{dX_{\rm hot}}{d\tau} = -X_{\rm hot}(1 - X_{\rm cold} - X_{\rm hot}) + BX_{\rm cold}X_{\rm hot}^2 , \quad (13)$$

with parameters A and B listed in Table 1. According to these equations, the time variation of the cold gas fractional mass $X_{\rm cold}$ is calculated to obtain the efficiency of the heavy-element accretion onto dust grains (eq. [8]).

Next, the time variation of the dust-to-gas ratio is solved. Since we are interested in a timescale much shorter than $\tau_{\rm SF}$, which is also interpreted as metal-production timescale through equation (6), we treat the values of X_i as constants. Then, equation (7) is solved for oxygen abundance (i = O, because we adopted oxygen as a tracer element in the previous work, H99; see also Lisenfeld & Ferrara 1998):

$$c\tau_{\rm SF}\frac{d\mathscr{D}_{\rm O}}{d\tau} = f_{\rm in,\,O}(\mathscr{R}X_{\rm O} + \mathscr{Y}_{\rm O}) - [\mathscr{R} - \beta_{\rm acc}(1 - f_{\rm O}) + \beta_{\rm SN}]\mathscr{D}_{\rm O} , \quad (14)$$

where we express the time in a nondimensional manner by using $\tau = ct$ and we assume $\alpha = 1$ (equivalent to the assumption that only dust incorporated into stars is destroyed in the star formation processes; § 2.1). We note the relation $f_{\rm O} = \mathscr{D}_{\rm O}/X_{\rm O}$. We fix the parameters as $\tau_{\rm SF} = 3 \times 10^9$ yr (e.g., Kennicutt et al. 1994), $f_{\rm in,O} = 0.05$ (H99), $\mathscr{R} = 0.79$, $\mathscr{Y}_{\rm O} = 1.8 \times 10^{-2}$, and $\beta_{\rm grow} = 100$ (corresponding to $\tau_{\rm grow} = \tau_{\rm SF}/100 = 3 \times 10^7$ yr); we note that $\beta_{\rm grow}$ and $\beta_{\rm acc}$ are related through eq. [8]), $\beta_{\rm SN} = 10$ (H99), and $X_{\rm O} = 0.013$ (the solar system abundance). The dependence on these parameters above, except for c and $\tau_{\rm SF}$, is described in Lisenfeld & Ferrara (1998), H99, and Hirashita (1999c). The parameter c scales the phase transition timescale, and we examine the cases of $c\tau_{\rm SF} = 100$ and 1000 (Table 1: $c^{-1} = 3 \times 10^6$–3×10^7 yr; IT83). We note that c appears in the form of the nondimensional parameter $c\tau_{\rm SF}$. We examine only the case of $c\tau_{\rm SF} = 100$ in models 1 and 2, since the qualitative behavior of the dust-to-gas ratio is the same, irrespective of which value of $c\tau_{\rm SF}$ is adopted.

Finally, the total dust-to-gas ratio $\mathscr{D}$ is calculated from the following equation:

$$\mathscr{D} = C\mathscr{D}_{\rm O} , \quad (15)$$

where we assume $C = 2.2$ (the Galactic value; Whittet 1992, p. 52).

We solve the basic equations (12)–(15) for the parameters listed in Table 1. The initial conditions for the filling factors are set according to IT83: $(X_{\rm cold}, X_{\rm hot}) = (0.0, 0.1)$ except for model 4 and $(X_{\rm cold}, X_{\rm hot}) = (0.0, 0.7)$ for model 4. The initial dust-to-gas ratio is set as $\mathscr{D} = 0.0080$ (Galactic value; Whittet 1992) for all the models. Models 3 and 4 are examined for two different values of c, listed in Table 1.

TABLE 1

EXAMINED MODELS

Model	A	B	$c\tau_{\rm SF}$	Type
1	1.2	3.0	100	Runaway
2	0.4	3.0	100	Stationary
3a	0.3	3.0	100	Limit-Cycle
3b	0.3	3.0	1000	Limit-Cycle
4a	0.3	0.5	100	Limit-Cycle
4b	0.3	0.5	1000	Limit-Cycle

[3] Two cases for each model are examined for different values of c, as explained in § 2.3 (models 3a, 3b, 4a, and 4b).

3. RESULTS

First, the result of model 1 is displayed in Figure 1. Because the cold gas disappears, the dust growth becomes ineffective. Then the dust destruction makes the dust-to-gas ratio converge to ~ 0 in the dust destruction timescale ($\sim 3 \times 10^8$ yr, i.e., 10 in units of c^{-1}). This model represents

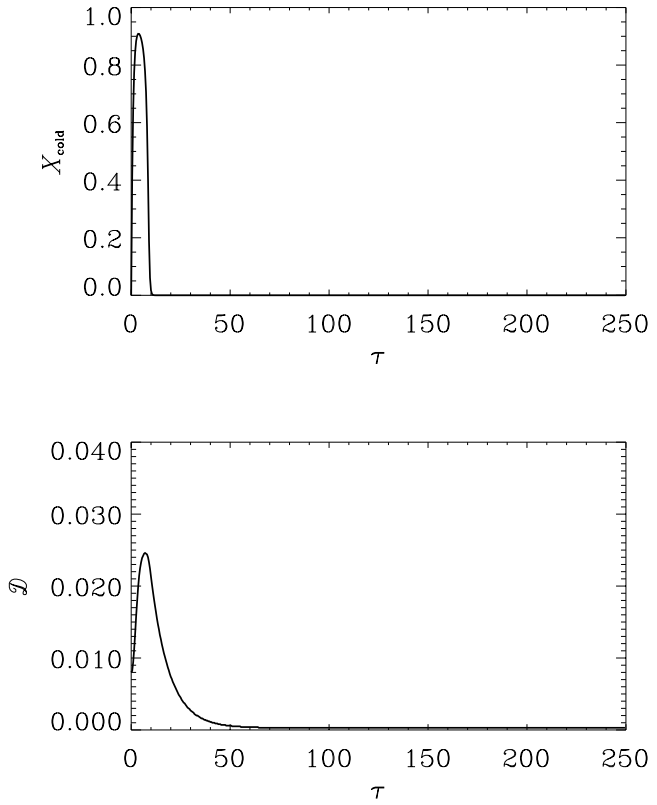

FIG. 1.—*Top*: Time evolution of the cold gas mass filling factor ($X_{\rm cold}$) for model 1. The initial condition is ($X_{\rm cold}$, $X_{\rm hot}$) = (0.0, 0.1). The adopted values of the parameters are $A = 1.2$, $B = 3.0$, and $c\tau_{\rm SF} = 100$. The time step is normalized by $c^{-1} \simeq 3 \times 10^7$ yr. *Bottom*: Time evolution of the dust-to-gas ratio ($\mathscr{D}$).

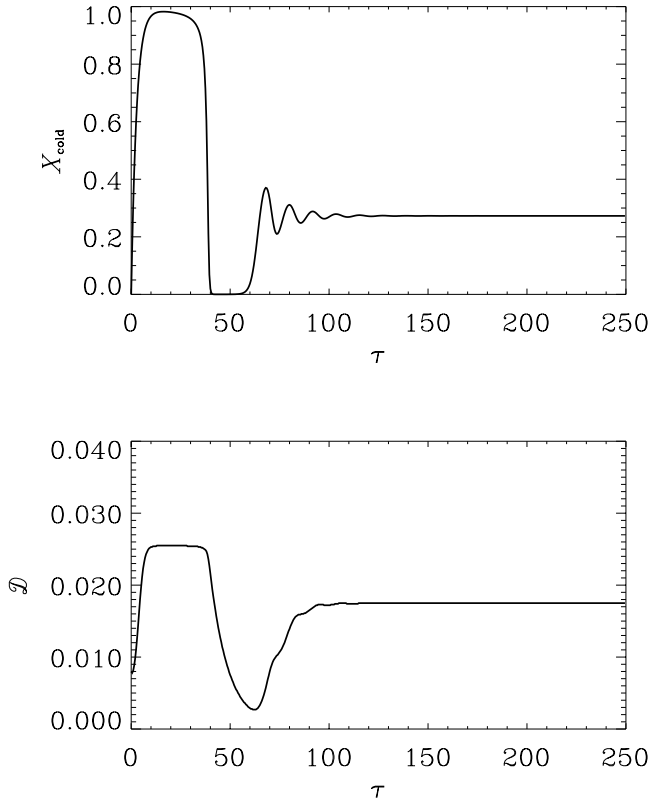

FIG. 2.—Same as Fig. 1, but for model 2. The initial condition is ($X_{\rm cold}$, $X_{\rm hot}$) = (0.0, 0.1). The adopted values of the parameters are $A = 0.4$, $B = 3.0$, and $c\tau_{\rm SF} = 100$. The time step is normalized by $c^{-1} \simeq 3 \times 10^7$ yr.

the efficient sweeping of warm gas in comparison with the radiative cooling of the hot gas. Thus, the swept gas is converted first into the cold component and then into hot gas (IT83). If the hot gas escapes out of the galaxy owing to its large thermal energy, this model corresponds to the galactic wind model of elliptical galaxies (IT83; Arimoto & Yoshii 1987).

The final value of the dust-to-gas ratio in model 1 is calculated by considering a stationary state, $d\mathscr{D}_{\rm O}/dt = 0$, in equation (14):

$$\frac{\beta_{\rm acc}}{X_{\rm O}}\mathscr{D}_{\rm O}^2 + (\mathscr{R} - \beta_{\rm acc} + \beta_{\rm SN})\mathscr{D}_{\rm O} - f_{\rm in,\,O}(\mathscr{R}X_{\rm O} + \mathscr{Y}_{\rm O}) = 0\ . \tag{16}$$

Because of the constant dust formation from metal injection at the rate of $f_{\rm in,O}(\mathscr{R}X_{\rm O} + \mathscr{Y}_{\rm O})$, the dust-to-gas ratio is not exactly 0 even after a long time. Since $X_{\rm cold} = 0$, $\beta_{\rm acc} = 0$. Thus, the solution of equation (16) is

$$\mathscr{D} = C\mathscr{D}_{\rm O} = \frac{Cf_{\rm in,\,O}(\mathscr{R}X_{\rm O} + \mathscr{Y}_{\rm O})}{\mathscr{R} + \beta_{\rm SN}} = 3 \times 10^{-4}\ , \tag{17}$$

for the adopted parameters $X_{\rm O} = 0.013$, $f_{\rm in,O} = 0.05$, $\mathscr{R} = 0.79$, $\mathscr{Y}_{\rm O} = 0.018$, and $\beta_{\rm SN} = 10$. This indeed matches the final value of the dust-to-gas ratio in model 1.

Next, the result of model 2 is presented in Figure 2. As shown in IT83, the solution for $X_{\rm cold}$ reduces to a stable point $(1 - A)/(AB + 1) = 0.27$. The stable stationary state is realized at a finite dust-to-gas ratio, which is determined so that the dust formation rate is balanced with the dust destruction rate. The value is calculated from equation (16). Using the adopted parameters, the positive solution is $\mathscr{D} = C\mathscr{D}_{\rm O} \simeq 0.017$, which matches the stationary value in Figure 2.

Finally, the limit-cycle case is examined in Figures 3 and 4. The four sets of parameters listed in Table 1 are examined (models 3a, 3b, 4a, and 4b). The resulting time evolution of the cold component of ISM and the dust-to-gas ratio is presented in Figures 3*a*, 3*b*, 4*a*, and 4*b* for the four cases. As expected, the dust-to-gas ratio oscillates in response to the fractional mass of the cold component, though the amplitude of the variation largely depends on the parameters. Comparing Figures 3*a* and 4*a* (or Figs. 3*b* and 4*b*), we see that the amplitude becomes larger if the period of the oscillation is longer. This is because the dust has enough time to grow if the period is long. Also from the comparison between the Figures 3*a* and 3*b* (or Figs. 4*a* and 4*b*), we find that the smaller c makes the amplitude larger. Since small c means that a time step of the phase transition model (eqs. [10] and [11]) is long in the real time unit ($\tau = 1$ corresponds to $t = c^{-1}$), the dust has enough time to grow in the case of smaller c. The timescale of the dust growth relative to that of the phase transition determines the amplitude. This point is discussed again in the next section.

4. DISCUSSIONS

4.1. *Timescales*

In the runaway and stationary solutions (models 1 and 2), the dust-to-gas ratio is settled into a stationary value determined by equation (16) after the dust formation and destruction timescales ($\sim 10^8$ yr). In the limit-cycle type solutions (models 3 and 4), the amplitude of the dust-to-gas

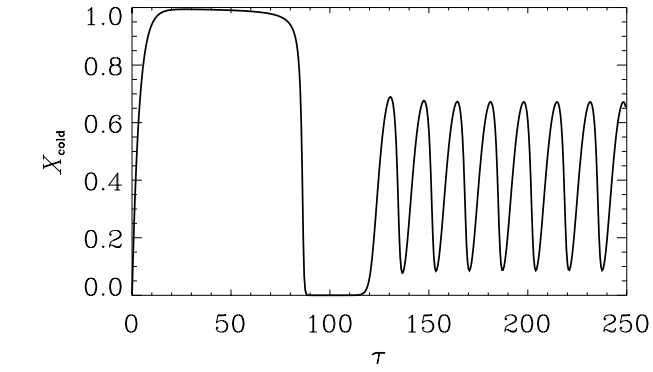

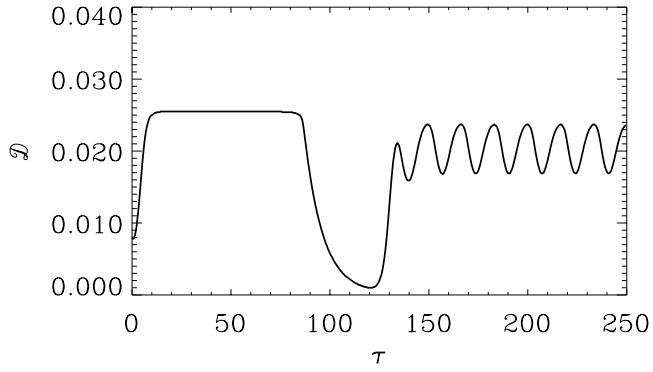

FIG. 3*a*

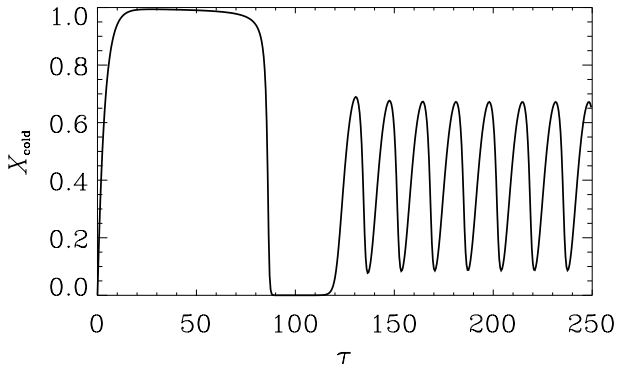

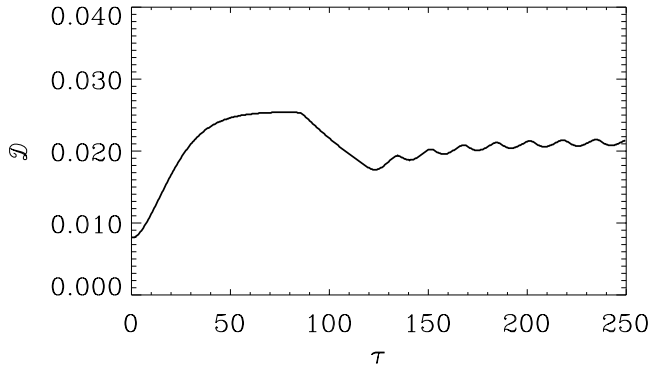

FIG. 3*b*

FIG. 3.—(*a*) Same as Fig. 1, but for model 3a. The initial condition is $(X_{\rm cold}, X_{\rm hot}) = (0.0, 0.1)$. The adopted values of the parameters are $A = 0.3$, $B = 3.0$, and $c\tau_{\rm SF} = 100$. The time step is normalized by $c^{-1} \simeq 3 \times 10^7$ yr. (*b*) Same as Fig. 1, but for model 3b. The initial condition is $(X_{\rm cold}, X_{\rm hot}) = (0.0, 0.1)$. The adopted values of the parameters are $A = 0.3$, $B = 3.0$, and $c\tau_{\rm SF} = 1000$. The time step is normalized by $c^{-1} \simeq 3 \times 10^6$ yr.

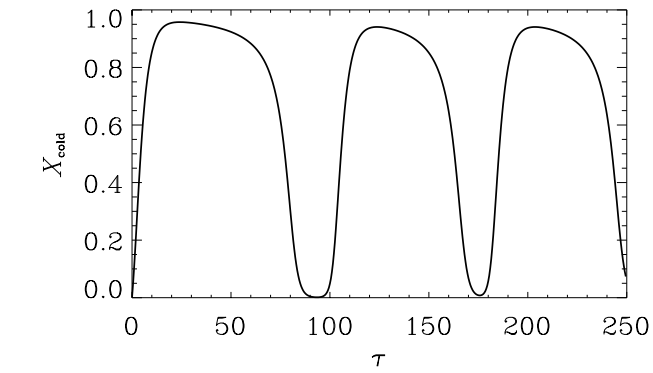

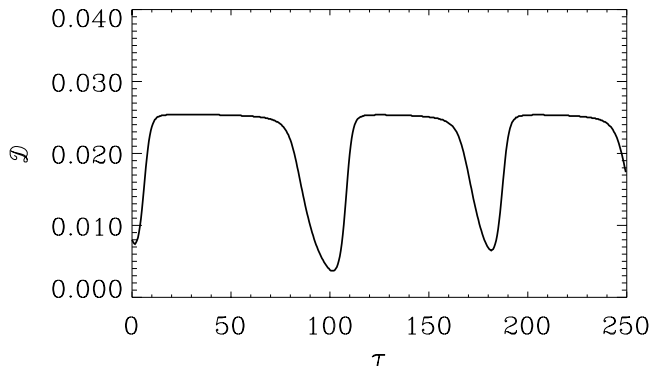

FIG. 4*a*

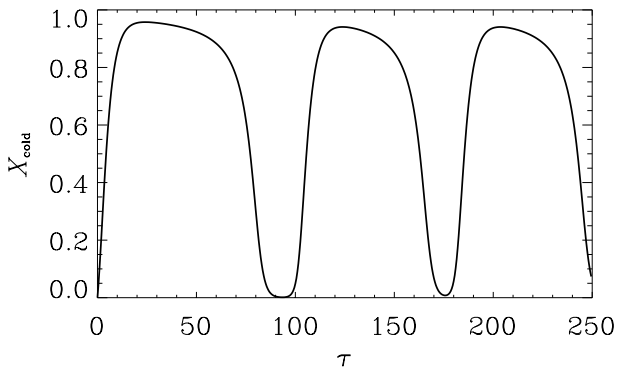

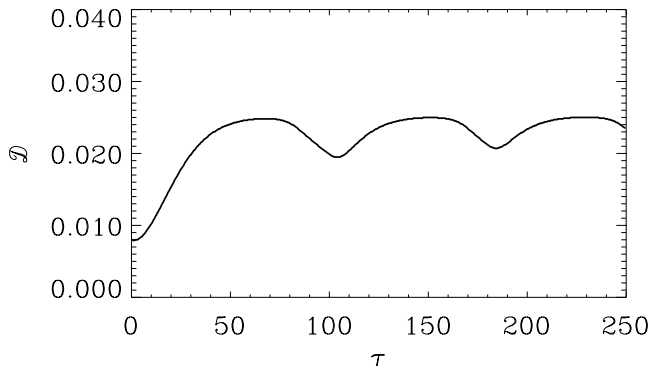

FIG. 4*b*

FIG. 4.—(*a*) Same as Fig. 1, but for model 4a. The initial condition is $(X_{\rm cold}, X_{\rm hot}) = (0.0, 0.7)$. The adopted values of the parameters are $A = 0.3$, $B = 0.5$, and $c\tau_{\rm SF} = 100$. The time step is normalized by $c^{-1} \simeq 3 \times 10^7$ yr. (*b*) Same as Fig. 1, but for model 4b. The initial condition is $(X_{\rm cold}, X_{\rm hot}) = (0.0, 0.7)$. The adopted values of the parameters are $A = 0.3$, $B = 0.5$, and $c\tau_{\rm SF} = 1000$. The time step is normalized by $c^{-1} \simeq 3 \times 10^6$ yr.

oscillation largely depends on the timescale of the phase transition. In this subsection, we discuss the phase transition and dust formation timescales in the limit-cycle model.

From the solution of the model equations in the previous section (Figs. 3 and 4), we find that the dust-to-gas ratio oscillates in response to the filling factor of the cold component. However, the amplitude of the oscillation is highly dependent on the values of the parameters A, B, and c. In other words, the amplitude is determined by the relation between the timescale of the phase transition (or the period of the oscillation) and that of the dust growth timescale. In the following, we discuss the relation between the period of the phase transition (denoted by $\tau_{\rm tr}$) and the dust growth timescale ($\tau_{\rm grow}$).

In order for the dust to grow, the dust must have enough time for the growth, i.e., $\tau_{\rm acc} < \tau_{\rm tr}$. By using equation (8), we find the condition is equivalent to

$$\frac{\tau_{\rm grow}}{X_{\rm cold}} < \tau_{\rm tr} , \tag{18}$$

which reads the following inequality by using $\beta_{\rm grow}$:

$$\frac{\tau_{\rm tr}}{\tau_{\rm SF}} > \frac{1}{\beta_{\rm grow} X_{\rm cold}} . \tag{19}$$

Putting $\beta_{\rm grow} = 100$ and $X_{\rm cold} = 0.5$, we obtain $\tau_{\rm tr}/\tau_{\rm SF} > 1/50$ for sufficient dust growth, which realizes the large amplitude of the time variation of the dust-to-gas ratio. This means that the timescale of the phase transition should be larger than several $\times 10^7$ yr for sufficient dust growth, since $\tau_{\rm SF} \sim 3$ Gyr (Kennicutt et al. 1994). Here, we note that the time step in Figures 3 and 4 is c^{-1} in the physical unit and that $c^{-1} = 3 \times 10^6$–3×10^7 yr. In the longer unit ($c^{-1} = 3 \times 10^7$ yr, corresponding to Figs. 3*a* and 4*a*), the amplitude of the dust-to-gas ratio oscillation is large. On the contrary, in the shorter unit ($c^{-1} = 3 \times 10^6$ yr; corresponding to Figs. 3*b* and 4*b*), the amplitude is much smaller, because the time step is shorter and thus condition (19) is not satisfied. Moreover, comparing Figures 3*a* and 4*a*, we see that the amplitude is larger if the period is longer.

In Figure 4*a*, the maximum of the dust-to-gas ratio is an order of magnitude larger than the minimum. Thus, the dust-to-gas ratio in spiral galaxies can show an order-of-magnitude oscillation. We should note that the parameter range is reasonable for the spiral galaxies (Ikeuchi 1988). Thus, we have confirmed the interpretation of the scatter of the dust-to-gas ratio that we presented in Hirashita (1999b), where we interpreted the scatter of the dust-to-gas ratio of the nearby spiral sample as the short-term ($\sim 10^7$–10^8 yr) variation of the dust-to-gas ratio with a maximum-to-minimum ratio of more than 4.

The important point is that the dust-to-gas ratio oscillation with large amplitude occurs in a reasonable parameter range for spiral galaxies (model 4a). However, the amplitudes are small for the other models after the stable limit cycle is attained. Thus, some spiral galaxies may not experience the prominent oscillation of the dust-to-gas ratio. But it is possible for the spiral galaxies to experience the oscillation of the dust-to-gas ratio, which is observed in the scatter of the dust-to-gas ratio of the spiral sample.

4.2. *Effect of Chemical Evolution*

In the discussions above, the metallicity was fixed because the timescale of the phase transition is much shorter than that of the chemical enrichment. However, the time range shown in the figures in this paper (250 time steps) corresponds to 7.5 Gyr when the $c\tau_{\rm SF} = 100$ is adopted. Thus, we need to examine the effect of the chemical evolution here.

To include the effect of chemical evolution, we solve equation (6) to examine the time variation of metallicity. If $\tau_{\rm SF}$ is fixed for simplicity, the solution to equation (6) becomes

$$X_{\rm O} = \frac{\mathcal{Y}_{\rm O}\tau}{c\tau_{\rm SF}} . \tag{20}$$

In other words, we simply assume a constant rate of metal enrichment to examine the effect of the chemical evolution qualitatively. We solve basic equations in § 2.3 for the time variable $X_{\rm O}$ described by equation (20). As a representative case, we adopt the parameter set identical to model 4a in Table 1, since the oscillation behavior of the dust-to-gas ratio is the most prominent (Fig. 4*a*). The result is shown in Figure 5. We see that the qualitative behavior of the dust-to-gas ratio is the same as the results for constant metallicity, except for the gradual increase of the dust-to-gas ratio. This increase is due to the metal production, from which dust is formed.

Thus, two behaviors of the temporal variation are coupled: one is the gradual increase of the dust-to-gas ratio on the timescale of chemical enrichment, and the other is the short-term variation of the dust-to-gas ratio owing to the ISM phase changes.

We note that the effect of chemical evolution is of significant importance if $\tau_{\rm SF}$ ($\sim$timescale of the chemical enrichment) is short. Especially for starburst galaxies, $\tau_{\rm SF} \sim 10^8$ yr, which is comparable to $\tau_{\rm tr}$ (Moorwood 1996). In this case, the metal enrichment also proceeds from the starburst in $\tau_{\rm SF}$, and thus the assumption of constant metallicity is never satisfied. The same discussion may also be applied to the initial burst in the formation epoch of galaxies, when $\tau_{\rm SF}$ is nearly the value of starburst galaxies ($\sim 10^8$ yr, the dynamical time).

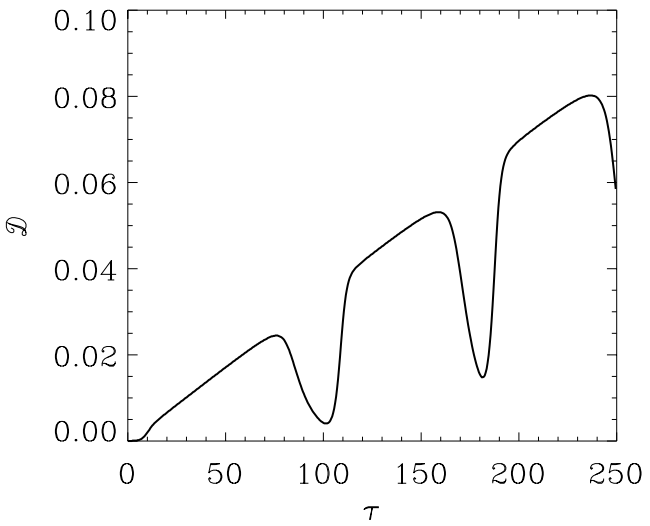

FIG. 5.—Time evolution of the dust-to-gas ratio. The model parameters are same as Fig. 4*a*, but the effect of the chemical evolution is included. A constant rate of metal enrichment is assumed.

4.3. *Observational Implications*

We have shown that the dust-to-gas ratio varies on a timescale of the ISM phase transition ($\sim 10^7$–10^8 yr) in spiral galaxies. The amplitude of the variation can be an order of magnitude (Figs. 3*a*–3*d*). This confirms the previous suggestion in Hirashita (1999b) that the dust-to-gas ratio scatter of the nearby spiral galaxies is explained by the time variation. The result also suggests that the variation is partially responsible for the scatter of the FIR-to-optical flux ratio of spiral sample in Tomita et al. (1996), since the dust content, as well as the stellar heating (dust temperature), is responsible for the far-infrared luminosity (e.g., Whittet 1992, p. 170).

We comment on the dust content in dwarf galaxies. Lisenfeld & Ferrara (1998) modeled the time evolution of the amount of dust in star-forming dwarf galaxies (dwarf irregular galaxies and blue compact dwarf galaxies). Based on their model and considering the dust formation in cold clouds (Dwek 1998), Hirashita (1999c) presented the hypothesis that in dwarf galaxies the dust growth is negligible compared with the dust condensation from metal ejected by stars. This is because the metallicities of dwarf galaxies are much smaller than those of spiral galaxies and collisions between grains and metal atoms are not frequent enough for efficient growth of the grains. Thus, the oscillation of the dust-to-gas ratio through the variation of the dust growth efficiency is difficult in dwarf galaxies. In this case, the scatter of the dust-to-gas ratio of the dwarf sample may be interpreted as reflecting the variable efficiency of the gas outflow (Lisenfeld & Ferrara 1998). The wind may easily blow out of the dwarf galaxies because of their shallow gravitational potentials (Larson 1974; De Young & Heckman 1994), though the distribution of dark matter largely affects the process of the outflow (Mac Low & Ferrara 1999; Ferrara & Tolstoy 2000).

We should note that the timescale of the phase transition in dwarf galaxies is expected to be longer because of their longer cooling timescales. Since metal-line cooling is the dominant cooling mechanism for the hot gas (Raymond, Cox, & Smith 1976), the small metallicity of dwarf galaxies, typically $\sim 1/10$ of that of the spiral galaxies, makes the cooling time an order of magnitude longer ($> 10^8$ yr). Thus, once the hot component becomes dominant in a dwarf galaxy, the dwarf galaxy must wait for the hot component to cool down for more than 10^8 yr, during which the growth of dust grains is prevented. This, as well as the mechanism in the previous paragraph, makes the dust growth difficult. Indeed, the dust-to-gas ratios in dwarf galaxies are known to be much smaller than those in spiral galaxies (e.g., Gondhalekar et al. 1986).

5. SUMMARY

We have discussed the time evolution of the dust-to-gas mass ratio in the context of multiphase models of interstellar medium in spiral galaxies. The phase transition of interstellar gas occurs on a timescale of $\sim 10^7$–10^8 yr in spiral galaxies (IT83). The dust growth rate also varies on that timescale, owing to the time variation of the fractional mass of the cold gas through the phase transition (Hirashita 1999b; § 2.1 of this paper). In order to examine the response of the dust-to-gas ratio to the phase transition, we modeled the time variation of the dust-to-gas ratio with a model of the phase transition. We adopt the three-phase model for the interstellar gas and the Ikeuchi-Tomita model for the phase transition. According to the model, three types of solutions are possible: (1) all the gas is transformed to a hot gas; (2) a stable stationary state of three phases is realized; and (3) the filling factors of each phase cyclically changes. For the three types of solutions, the dust-to-gas ratio behaves as follows (§ 3): for solution 1, the dust is fully destroyed (the dust-to-gas ratio becomes 0); for solution 2, the dust-to-gas ratio converges to a stationary state; and for solution 3 the dust-to-gas ratio varies cyclically in response to the phase transition. When case 3 is applicable, the amplitude of the variation of the dust-to-gas ratio is large (nearly an order of magnitude) if the dust growth timescale is shorter than the phase transition timescale. This condition is satisfied within the reasonable parameter range of spiral galaxies (§ 4.1).

However, the model needs to be modified for dwarf galaxies, since their small metallicity makes the dust growth rate in clouds small (Hirashita 1999c), and their timescale of the phase transition is longer owing to their longer cooling timescale. For starburst galaxies, the effect of chemical enrichment is important because of their short metal-enrichment timescale.

We wish to thank the anonymous referee for useful comments that substantially improved this paper. We are grateful to S. Mineshige for his continuous encouragement. This work is supported by the Research Fellowship of the Japan Society for the Promotion of Science for Young Scientists. We have made extensive use of NASA's Astrophysics Data System Abstract Service (ADS).

REFERENCES

Arimoto, N., & Yoshii, Y. 1987, A&A, 173, 23
Barlow, M. J. 1978, MNRAS, 183, 367
Borkowski, K. J., & Dwek, E. 1995, ApJ, 454, 254
De Young, D. S., & Heckman, T. M. 1994, ApJ, 431, 598
Draine, B. T. 1990, in Evolution of the Interstellar Medium, ed. L. Blitz (San Francisco: ASP), 193
Draine, B. T., & Salpeter, E. E. 1979, ApJ, 231, 438
Dwek, E. 1998, ApJ, 501, 643
Dwek, E., & Scalo, J. M. 1980, ApJ, 239, 193
Ferrara, A., & Tolstoy, E. 2000, MNRAS, submitted (astro-ph/9905280)
Fujimoto, M., & Ikeuchi, S. 1984, PASJ, 36, 319
Gondhalekar, P. M., Morgan, D. H., Dopita, M., & Ellis, R. S. 1986, MNRAS, 219, 505
Habe, A., & Ikeuchi, S. 1980, Prog. Theor. Phys., 64, 1995
Habe, A., Ikeuchi, S., & Tanaka, Y. D. 1981, PASJ, 33, 23
Hirashita, H. 1999a, ApJ, 510, L99 (H99)
Hirashita, H. 1999b, A&A, 344, L87
———. 1999c, ApJ, 522, 220
Ikeuchi, S. 1988, Fundam. Cosmic Phys., 12, 255
Ikeuchi, S., & Tomita, H. 1983, PASJ, 35, 77 (IT83)
Jones, A. P., Tielens, A. G. G. M., Hollenbach, D. J., & McKee, C. F. 1994, ApJ, 433, 797
Kamaya, H., & Takeuchi, T. T. 1997, PASJ, 49, 271 (KT97)
Kennicutt, R. C., Jr., Tamblyn, P., & Congdon, C. W. 1994, ApJ, 435, 22
Korchagin, V. I., Ryabtsev, A. D., & Vorobyov, E. I. 1994, Ap&SS, 220, 115
Larson, R. B. 1974, MNRAS, 169, 229
Lisenfeld, U., & Ferrara, A. 1998, ApJ, 496, 145
Mac Low, M.-M., & Ferrara, A. 1999, ApJ, 513, 142
McKee, C. F. 1989, in Interstellar Dust, ed. L. J. Allamandola & A. G. G. M. Tielens (Dordrecht: Kluwer), 431
McKee, C. F., Hollenbach, D. J., Seab, C. G., & Tielens, A. G. G. M. 1987, ApJ, 318, 674

McKee, C. F., & Ostriker, J. P. 1977, ApJ, 218, 148
Moorwood, A. F. M. 1996, Space Sci. Rev., 77, 303
Nicolis, G., & Prigogine, I. 1977, Self-Organization in Nonequilibrium Systems (New York: Wiley)
Raymond, J. C., Cox, D. P., & Smith, B. W. 1976, ApJ, 204, 290
Roberts, M. S. 1963, ARA&A, 1, 149
Schmidt, M. 1959, ApJ, 129, 243
Seab, C. G. 1987, in Interstellar Processes: Proceedings of the Symposium on Interstellar Processes, ed. D. J. Hollenbach & H. A. Thronson (Dordrecht: Reidel), 491
Takagi, T., Arimoto, N., & Vansevičius, V. 1999, ApJ, 523, 107
Tomita, A., Tomita, Y., & Saitō, M. 1996, PASJ, 48, 285
Wang, B. 1991, ApJ, 374, 456
Whittet, D. C. B. 1992, Dust in the Galactic Environment (New York: Inst. Phys.)